Modeling the Glucose Sensor Error

Andrea Facchinetti, Simone Del Favero, Giovanni Sparacino, Jessica R. Castle, W. Kenneth Ward, and Claudio Cobelli*, *Fellow, IEEE*

***Abstract*—Continuous glucose monitoring (CGM) sensors are portable devices, employed in the treatment of diabetes, able to measure glucose concentration in the interstitium almost continuously for several days. However, CGM sensors are not as accurate as standard blood glucose (BG) meters. Studies comparing CGM versus BG demonstrated that CGM is affected by distortion due to diffusion processes and by time-varying systematic under/overestimations due to calibrations and sensor drifts. In addition, measurement noise is also present in CGM data. A reliable model of the different components of CGM inaccuracy with respect to BG (briefly, "sensor error") is important in several applications, e.g., design of optimal digital filters for denoising of CGM data, real-time glucose prediction, insulin dosing, and artificial pancreas control algorithms. The aim of this paper is to propose an approach to describe CGM sensor error by exploiting n multiple simultaneous CGM recordings. The model of sensor error description includes a model of blood-to-interstitial glucose diffusion process, a linear time-varying model to account for calibration and sensor drift-in-time, and an autoregressive model to describe the additive measurement noise. Model orders and parameters are identified from the n simultaneous CGM sensor recordings and BG references. While the model is applicable to any CGM sensor, here, it is used on a database of 36 datasets of type 1 diabetic adults in which $n = 4$ Dexcom SEVEN Plus CGM time series and frequent BG references were available simultaneously. Results demonstrates that multiple simultaneous sensor data and proper modeling allow dissecting the sensor error into its different components, distinguishing those related to physiology from those related to technology.**

***Index Terms*—Continuous glucose monitoring, diabetes, measurement noise, parameter estimation, sensor calibration.**

I. Introduction

CONTINUOUS glucose monitoring (CGM) sensors are portable devices able to measure (and visualize in real time) glucose in the interstitium almost continuously (1–5 min sampling period) for several consecutive days (presently up to seven) [1]–[4]. CGM sensors have dramatically improved the treatment of type 1 diabetes [5]. The advent of CGM has allowed investigations that were previously not possible by the sparseness of self-monitoring blood glucose (SMBG) measurements. For instance, CGM data can be analyzed retrospectively, e.g., to evaluate blood glucose (BG) variability [6], [7] and the risk associated to the current glycemic value [8]–[10], but also used in real time to generate alerts when glucose crosses hypoglycemic or hyperglycemic thresholds [11]–[13]. An interesting development is the real-time prediction of future glucose concentration that allows preventing rather than simply detecting critical hypoglycemic and hyperglycemic episodes [14]–[16]. Finally, CGM sensors are key elements of an artificial pancreas (AP) [17], which represent a new frontier for the treatment and management of type 1 diabetes [18]–[22].

At present, CGM sensors are not as accurate as BG meters. In particular, studies comparing CGM versus BG references frequently measured via laboratory instruments [24], [25], showed the existence of several components of inaccuracy. A first discrepancy is a distortion due to blood-to-interstitium glucose kinetics (BG-to-IG), which results in a lag of some minutes. Then, systematic under/overestimations with time-varying amplitude are often present: these can be due either to errors in sensor calibration, e.g., timing or level of SMBG sample used for calibration, or to a drift-in-time of sensor sensitivity. Finally, CGM time series are corrupted by a random zero-mean measurement noise. These components of inaccuracy of CGM with respect to BG, which we briefly refer to as "sensor error," can be easily recognized by looking at Fig. 1, which shows BG references frequently collected every 15 min for 9 h (circles linearly interpolated by a straight line), and four CGM time series (other lines) measured simultaneously using the Dexcom SEVEN Plus glucose sensor [23]. For instance, the lag due to BG-to-IG kinetics is visible in sensor 1 during the rising front around time 90 min. A significant overestimation is present throughout the time-course of CGM sensors 3 and 4. Sensor 2 underestimates glucose concentration till time 260 min only, probably as a result of a drift-in-time of sensor sensitivity. Random zero-mean measurement noise is visible in all CGM time series, e.g., in sensor 1 in the time interval 100–150 min. In addition, the relative role of the different components of sensor error varies significantly among the four sensors.

A model of sensor error able to dissect the components of inaccuracy can be important in several applications. For instance, the availability of a reliable description of the zero-mean random measurement noise component can enable a better design of optimal (in a Bayesian sense) digital filters for denoising according to [26], [27]; a precise assessment of the BG-to-IG kinetics can render enhancement and calibration methods more effective [10], [28]; finally, an accurate sensor error model is crucial in the type 1 diabetes simulator [29], [30] to test *in silico* AP closed-loop control algorithms.

Two attempts to model the CGM sensor error have been published. In the model proposed by Breton and Kovatchev [31],

Manuscript received May 9, 2013; revised July 23, 2013; accepted September 20, 2013. Date of publication September 30, 2013; date of current version February 14, 2014. *Asterisk indicates corresponding author.*

A. Facchinetti, S. Del Favero, and G. Sparacino are with the Department of Information Engineering, University of Padova, 35131 Padova, Italy (e-mail: facchine@dei.unipd.it; sdelfave@dei.unipd.it; gianni@dei.unipd.it).

J. R. Castle and W. K. Ward are with the Department of Medicine, Oregon Health & Science University, Portland, OR 97239 USA (e-mail: castleje@ohsu.edu; wardwk@ohsu.edu).

*C. Cobelli is with the Department of Information Engineering, University of Padova, 35131 Padova, Italy (e-mail: cobelli@dei.unipd.it).

Digital Object Identifier 10.1109/TBME.2013.2284023

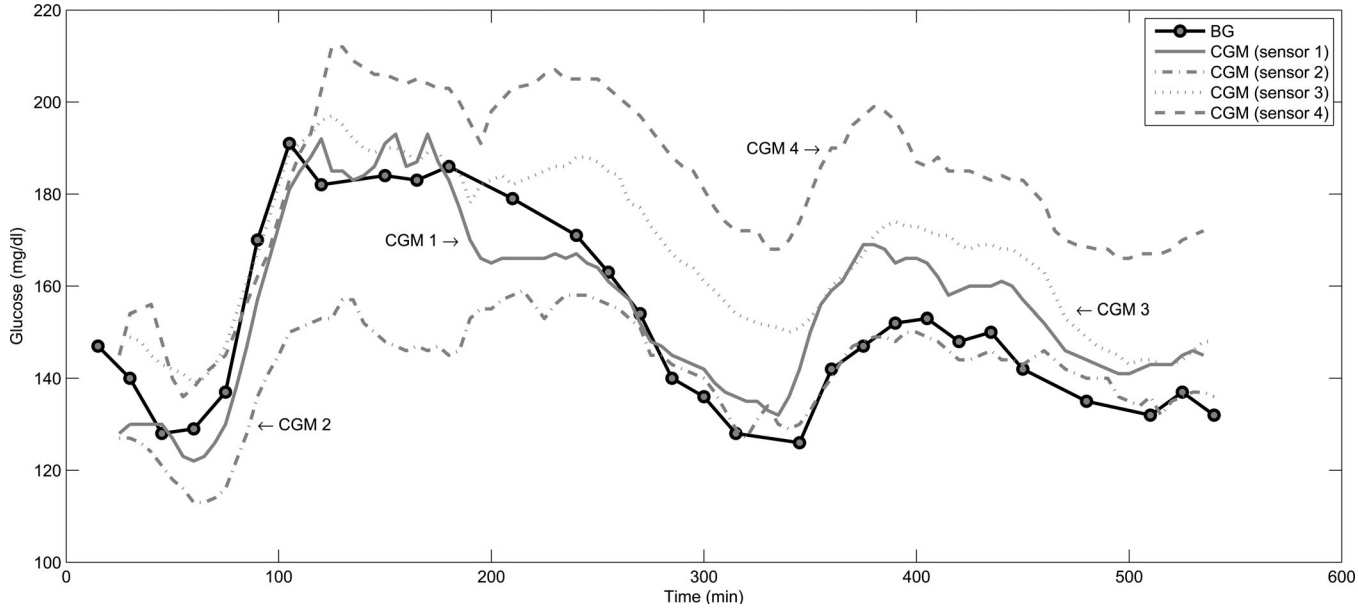

Fig. 1. Representative example of the dataset employed in this paper [23]. BG references frequently collected every 15 min for 9 h (circles linearly interpolated by a straight line), and CGM time series (other lines) measured simultaneously using $n = 4$ Dexcom SEVEN Plus glucose sensors in a type 1 diabetic individual.

errors due to calibration and BG-to-IG kinetics are first mitigated by *a posteriori* recalibration of CGM data using all available BG references (one every 15 min for about 40 h) and IG profile is estimated by feeding a first-order linear time-invariant dynamic model [32] with interpolated BG data (time constant of BG-to-IG kinetics model set to 17 min for all subjects); then, the residual profile, assumed representative of the sensor measurement error, is used to fit a first-order autoregressive (AR) model. This model was able to describe some of the random fluctuations visible on CGM experimental data, but it is suboptimal because it cannot describe errors due to calibration and sensor drift nor deal with interindividual variability of the BG-to-IG kinetics [33]. A second model was proposed by Lunn *et al.* [34] and can be considered a refinement of the first-order AR model of [31]. In fact, the time constant of BG-to-IG kinetics is individualized in each subject and a model to take into account errors due to suboptimal calibration is considered. Even if it improves the model of [31], it cannot cope with sensor drift (the incorporated recalibration function is time-invariant) and, similarly to [31], the residuals against which the AR model is fitted can also reflect some spurious dynamics induced by suboptimal modeling of either calibration or BG-to-IG kinetics.

In this paper, we propose a model which describes the different components responsible of CGM sensor inaccuracy. At variance from [31], [34], where only a single CGM time series was used, here, we take advantage of a database consisting of multiple simultaneous CGM readings and BG references (as in Fig. 1) which allows us dissect the overall CGM sensor error into its different components, in particular by distinguishing those related to physiology from those related to technology. While the method will be assessed on Dexcom SEVEN Plus CGM data, the proposed approach is general and can be used to describe the error of any commercial CGM sensor.

This paper outline is as follows. In Section II, we illustrate the database; Section III presents the formulation of the model for CGM sensor error; Section IV describes the method to identify the model parameters; in Section V results are discussed; finally, in Section VI, we draw some conclusions.

II. Database

The database used to test the approach is taken from [23] and consists of 19 patients with type 1 diabetes recruited from Oregon Health & Sciences University (OHSU) outpatient clinics in Portland. Cohort details, as well as information on inclusion and exclusion criteria, and approval of the study can be found in [23]. Each patient underwent two separate sessions, a total of 36 sessions were available. For each session, each patient wore four Dexcom SEVEN Plus glucose sensors, two placed to the right of the umbilicus and two to the left. The morning after the insertion, subjects were admitted to the Oregon Clinical & Translational Research Institute at OHSU for a 9-h study, during which venous glucose was measured every 15 min using a HemoCue Glucose 201 Analyzer. All four CGM sensors were calibrated with the same HemoCue reference value at the same time, i.e., just before the 9 h in hospital session. No further calibrations have been performed afterward.

III. Model

The general scheme of the n CGM data streams (here, $n = 4$) is described in Fig. 2. The BG concentration signal is transformed into IG concentration through BG-to-IG kinetics. We assume that in each individual the BG-to-IG kinetics is, in absence of external factors such as physical activity, the same for all n sensors. Hence, the IG signal is the same for all of the n CGM channels. Then, the IG signal is measured by each of the n CGM sensors, generating, for the ith sensor $(i = 1, \ldots, n)$,

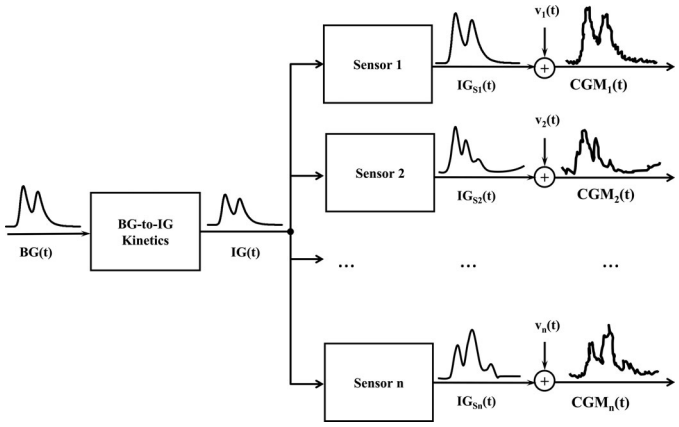

Fig. 2. Scheme describing how n simultaneous CGM data streams are modeled. From left to right: the BG signal is transformed into IG signal through the BG-to-IG kinetics; the IG signal is measured by each of the n CGM sensors, generating for the ith sensor the IG_{S_i} profile; finally, the measured CGM_i is affected by additive measurement noise v_i.

the IG_{S_i} profile. The IG_{S_i} are all different due to unpredictable effects of the specific sensor, e.g., different body reaction from site-to-site or different sensor drift in time. Finally, the output of each of the n CGM sensors, $\mathrm{CGM}_i(t)$, is affected by additive measurement noise $v_i(t)$

$$\mathrm{CGM}_i(t) = \mathrm{IG}_{S_i}(t) + v_i(t). \tag{1}$$

Let us now describe in detail the three steps of Fig. 2.

1) The first is to model the BG-to-IG diffusion process and we use the compartmental model proposed by Rebrin *et al.* [32]. Given the first-order model, by assuming that kinetics are linear and parameters time-invariant, and that the static gain of the system is equal to 1 (i.e., in steady state, BG and IG are equal), BG and IG concentrations are related by a convolution equation

$$\mathrm{IG}(t) = h(t) * \mathrm{BG}(t) \tag{2}$$

where

$$h(t) = \frac{1}{\tau} e^{-t/\tau} \tag{3}$$

is the impulse response of the BG-to-IG system. The parameter τ is the time constant of the system and will be identified in each individual from the data as described later in Section IV. The description of (2)–(3), although simple, is currently the most used in the literature, see, e.g., [28], [31], [34], [35].

2) The second step is to describe how the ith sensor converts the "true" IG in a measurable quantity IG_{S_i}, where S stands for sensor and i indicates the sensor number. Physically, using the glucose-oxidase principle the CGM sensor measures a raw current, proportional to the IG concentration, which is then transformed into glucose values with a first-order linear regression calibration function. The calibration process can be suboptimal (e.g., because of errors in the BG data used as reference) and, in addition, a significant drift in time (e.g., due to a modification of the sensitivity of the sensor during the monitoring) can be present (see Fig. 1). To take into account these factors, the relationship between IG_{S_i} and $\mathrm{IG}(t)$ is described as

$$\mathrm{IG}_{S_i}(t) = a_i(t)\mathrm{IG}(t) + b_i(t) \tag{4}$$

where $a_i(t)$ and $b_i(t)$ are, respectively, time-varying gain and offset parameters of the ith sensor. Several models for $a_i(t)$ and $b_i(t)$ can be used. Since no *a priori* information on their evolution in time is available, a flexible description is that given by polynomials

$$a_i(t) = \sum_{k=0}^{m} a_{ik} t^k \tag{5}$$

$$b_i(t) = \sum_{k=0}^{l} b_{ik} t^k \tag{6}$$

where the orders m and l are model parameters that will be determined from the data as described in Section IV (a set of values for each sensor and for each individual). Note that allowing the time variance of $a_i(t)$ and $b_i(t)$ is a novelty with respect to the previous attempts [31], [34].

Remark: The model assumes piecewise constant parameters m, l, a_{ik}, and b_{ik} of the calibration error model [see (5) and (6)] between two consecutive calibrations. This choice is imposed by the present dataset, which presents 9 h of monitoring with no sensor calibrations within this time window.

3) The third step describes the zero-mean random measurement noise $v_i(t)$ affecting the ith CGM signal. We assume it additive and, according to the evidences on autocorrelation reported in both [31], [34], described by an AR process of order q

$$v_i(t) = \sum_{k=1}^{q} \alpha_{ik} v_i(t-k) + w_i(t) \tag{7}$$

with $w_i(t) = \mathcal{N}(0, \sigma^2_{w_i})$. Model parameters α_{ik} and $\sigma^2_{w_i}$, and order q will be determined, for each of the n sensor signals, as described in the following Section IV.

IV. Identification

The identification of the parameters of the submodels described in Section III is performed in two steps. First, the time constant τ of (3) and the optimal orders m and l of the calibration parameters a_i, b_i (for $i = 1, \ldots, n$) of (5) are determined. Then, the order q and the parameters of (7) are estimated.

In the first step, the selection of optimal orders m and l of the polynomials $a(t)$ and $b(t)$ of the calibration function is performed by minimizing the Bayesian information criterion (BIC) index

$$\mathrm{BIC} = d\ln(\mathrm{RSS}) + p\ln(d) \tag{8}$$

where d is the total number of CGM data available in each individual from all the sensors, $p = (m + l + 2)$ is the number of parameters of the model, and RSS is the residual sum of squares computed as

$$\mathrm{RSS} = \sum_{i=1}^{n} \sum_{j=1}^{d_i} \nu_{ij}^2 \tag{9}$$

in which ν is the uncorrelated version of v (a whitening filter is used to correctly use BIC) and d_i is the number of CGM samples of sensor i. The BIC index takes into account both the statistical goodness of fit [first part of (8)] and the number of parameters that have to be estimated [second part of (8)], by imposing a penalty for increasing the number of parameters. When comparing different models, the model with the lower value of BIC is the one to be preferred. Several combinations of m and l need to be tested to verify which one better describes the data. In this paper, for sake of readability, we consider only the following four candidate combinations: $m = l = 0$ (*"constant"*), as in [31] and [34] where parameters are assumed to be time invariant (i.e., no drift in time); $m = l = 1$ (*"linear"*), i.e., both the gain and the offset vary in time following a linear trajectory; $m = l = 2$ (*"quadratic"*), i.e., a quadratic time evolution is considered; $m = l = 3$ (*"cubic"*), i.e., time variations obey to a cubic law (the use combinations with $m \neq l$ will be discussed in Section V-A). For each combination of m and l, the identification of the other parameters, i.e., τ and the coefficients of the polynomials $a_i(t)$ and $b_i(t)$ is performed by nonlinear least squares. The outputs are a numerical value $\hat{\tau}$, the integers m and l, which give the orders of the polynomial functions $a_i(t)$ and $b_i(t)$ $(i = 1, \ldots, n)$ of (5), and their parameters values $\hat{a}_{i1}, \ldots, \hat{a}_{im}, \hat{b}_{i1}, \ldots, \hat{b}_{il}$ (a set of values for each sensor and for each individual).

In the second step, the zero-mean random measurement noise model is identified. First, the residual profile $\text{res}_i(t)$ is computed

$$\text{res}_i(t) = \text{CGM}_i(t) - \left(\sum_{k=0}^{m} \hat{a}_{ik} t^k \left(\frac{1}{\hat{\tau}} e^{-t/\hat{\tau}} * \text{BG}(t) \right) + \sum_{k=0}^{l} \hat{b}_{ik} t^k \right). \tag{10}$$

This profile represents what remains unexplained in the CGM data by using the reference BG through and previously identified models of BG-to-IG kinetics and sensor calibration. Because of possible suboptimal modeling of the physiological BG-to-IG diffusion process and calibration, the residual profile $\text{res}_i(t)$ contains some dynamics not explained by the models, meaning that $\text{res}_i(t)$ cannot be in general considered as reflecting zero-mean random measurement noise only. Differently from [31], [34], the availability of multiple sensor data allows us to check if additional components are indeed present. To do so, assuming that the measurement noise v_i is uncorrelated from v_j, with $i \neq j$, we perform a correlation analysis among $\text{res}_i(t)$ profiles. If a significant correlation is present, it is concluded that residuals contain components other than measurement noise and we calculate what we label as "common component" as

$$\text{cc}(t) = \frac{1}{n} \sum_{i=1}^{n} \text{res}_i(t). \tag{11}$$

If detected on the data, this component can be modeled as an AR process, whose order will be selected again resorting to BIC. Finally, an estimate of the realization of the random measurement noise $v_i(t)$ of Fig. 2 is, first, calculated as

$$\hat{v}_i(t) = \text{res}_i(t) - \text{cc}(t) \tag{12}$$

and, then, fitted by an AR process of order q, as in (7), by using least squares.

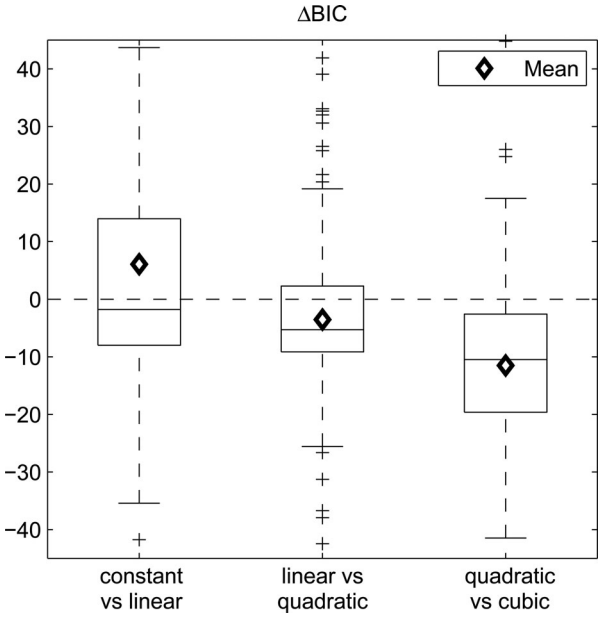

Fig. 3. Boxplots of ΔBIC values obtained in the determination of the orders m and l of the polynomials $a_i(t)$ and $b_i(t)$ of the calibration error function: constant versus linear (Left), linear versus quadratic (Middle), and quadratic versus cubic (Right). The diamond ($\diamond$) represents the mean value. A positive value of ΔBIC means that the higher order is preferable.

V. Results

A. Order Selection of Polynomials $a_i(t)$ and $b_i(t)$

Fig. 3 shows a summary of the results by depicting the boxplots of the differences in BIC values (ΔBIC) between all the possible pairs of combinations (*constant* versus *linear*, *linear* versus *quadratic*, and *quadratic* versus *cubic*). Given two combinations, e.g., *constant* versus *linear*, ΔBIC is calculated as BIC of the *constant* combination minus BIC of the *linear* combination. As a consequence, a positive difference in ΔBIC means that the higher order model performs better than the lower one. As visible on the boxplot on the left, the introduction of a linear term is positive in about 50% of the cases, with an average $\Delta\text{BIC} = 6.1$. This result can be interpreted as follow: in half of the cases, no or limited drift on the data is present; however in the other half, the drift is so marked that the explanatory benefit of introducing a linear degree of freedom overcomes the penalty we assess for the extra complexity, suggesting that *linear* approximation is more reliable than the *constant* one. Moving to the boxplot in the middle, the introduction of the quadratic term is not advantageous, since the mean is negative ($\Delta\text{BIC} = -3.5$) and the number of traces in which the introduction of the quadratic term leads to positive effect is about 29% of the cases only. Finally, focusing on the boxplot on the right, we can also see that the introduction of a cubic term is not beneficial, being the average ΔBIC even negative than in the previous case ($\Delta\text{BIC} = -11.5$) and being lower than 25% the number of traces in which the introduction of the cubic term leads to a

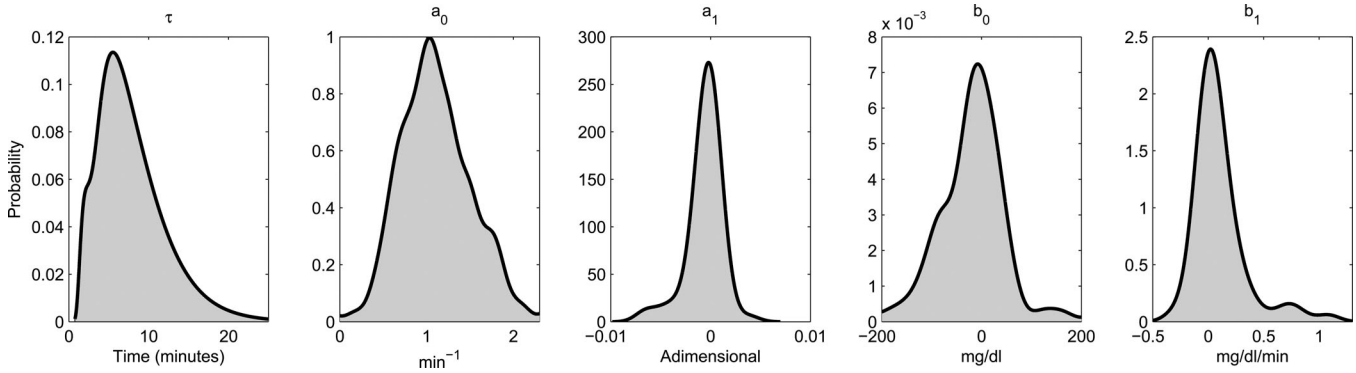

Fig. 4. Probability density functions of parameters τ, a_0, a_1, b_0, and b_1 obtained from estimated values and through a kernel density estimation procedure.

TABLE I
MEDIAN, 5TH AND 95TH PERCENTILES VALUES FOR MODEL PARAMETERS $\hat{\tau}$, $\hat{a}_0$, $\hat{a}_1$, $\hat{b}_0$, $\hat{b}_1$, AND PERCENTAGE OF VALUES ESTIMATED WITH A COEFFICIENT OF VARIATION CV $\leq 10\%$ AND CV $\leq 30\%$

	Percentile			% of values estimate with	
Parameter	50^{th}	5^{th}	95^{th}	$CV < 10\%$	$CV < 30\%$
$\hat{\tau}$	6.7	2.2	12.5	97%	97%
$\hat{a}_0$	1.1	0.5	2.4	100%	100%
$\hat{a}_1$	0.0002	-0.0044	0.0012	79%	94%
$\hat{b}_0$	-14.8	-225.9	63.4	83%	95%
$\hat{b}_1$	0.04	-0,14	0.70	77%	94%

positive effect. From this analysis, we can conclude that $m = 1$ and $l = 1$, i.e., the introduction of a linear term in both gain and offset descriptions seems the best choice to explain the data.

Remark: we also investigated cases with $m \neq l$. However, they were less interesting, at least for the present dataset. In fact, even if ΔBIC distributions, calculated by comparing the *constant* setting versus $(m = 0, l = 1)$ and $(m = 1, l = 0)$, are similar to that of *constant versus linear* scenario of Fig. 3 (data not shown), the average ΔBIC values (4.5 and 5.6, respectively) are lower than the $\Delta\text{BIC} = 6.1$ obtained with the *linear* case. Furthermore, the *linear* case has a higher ΔBIC individual value. These observations suggest that the greater benefit with respect to the *constant* scenario is given by the *linear* one. Similar considerations also hold when considering higher orders. However, since we cannot exclude that the time-varying component could be dataset and/or sensor specific, in general it is advisable to perform a preliminary study with all (m, l) combinations.

B. Parameters τ, a_0, a_1, b_0, and b_1

Fig. 4 shows, for the optimal orders $m = 1$ and $l = 1$, the distributions of $\hat{\tau}$, $\hat{a}_0$, $\hat{a}_1$, $\hat{b}_0$, and $\hat{b}_1$ obtained applying a kernel density estimation procedure on the whole dataset, while, to better understand values and ranges, Table I reports median, 5th, and 95th percentiles. Note that the distributions of Fig. 4 and the values in Table I are obtained by aggregating the results of all $n = 4$ sensors.

In order to better understand if the values estimated with this procedure are reliable, it is important to look at the precision of the estimates. To do so, first we calculated the coefficient of variation (CV) for the each of the estimated parameters, then we counted the number of parameters that were estimated with elevated precision, i.e., with CV $\leq 10\%$ and CV $\leq 30\%$, see the last two columns of Table I. Most of the parameters have been estimated with a good precision. In the specific, τ value has been precisely estimated (CV $\leq 5\%$) in all subjects but one, in which the BG references time series appeared to be delayed with respect of CGM data (probably due to an error in recording of temporal instants in which samples have been collected). To validate the goodness of these results, we also performed the estimation of τ for each time series individually, thus ignoring the availability of multiple sensors (mimicking what was done in [31] and [34]). Two interesting results have been obtained: first, the number of $\hat{\tau}$ values estimated with an elevated precision decreases to less than 80%, meaning that, without multiple sensor data, the estimation of the time constant of the BG-to-IG diffusion process is difficult; second, a significant intraindividual variability of τ emerges, e.g., in a single individual τ can range from 2 to 25 min, which appears to be unreliable. Thus, we can affirm that the estimation of τ is much more robust if multiple CGM sensors are available.

Some considerations on the estimated values are reported. Starting from time constant τ of the BG-to-IG diffusion process, we can note that the median value is 6.7 min, in line with values observed in a previous study employing the same sensor [12], [36]. However, as visible from both Fig. 4 and Table I, the interindividual variability of τ is large, with values spanning from 2.2 to 13.7 min. With regard to the coefficients of the gain $a(t)$ and offset $b(t)$ of the calibration error function, a significant variability in terms of gain ($\hat{a}_0$ from 0.5 to 2) and static offset ($\hat{b}_0$ from -226 to 63) is visible, evidencing that the calibration error plays a key role in the accuracy of the sensor. In addition, the estimation procedure highlights a significant variability of the coefficients of the first-order term, $\hat{a}_1$ and $\hat{b}_1$, meaning that a drift-in-time of the sensitivity of the sensor is present. Finally, we note that an elevated correlation exists among calibration function parameters ($r^2 > 0.78$ for all combinations), e.g., the correlation between a_0 and b_0 is $r = -0.95$, meaning that an elevated static gain is coupled with a very negative offset, and vice versa.

C. Measurement Noise Model

With regard to the residual analysis, the top panel of Fig. 5 shows the $n = 4$ raw residual profiles in the same representative

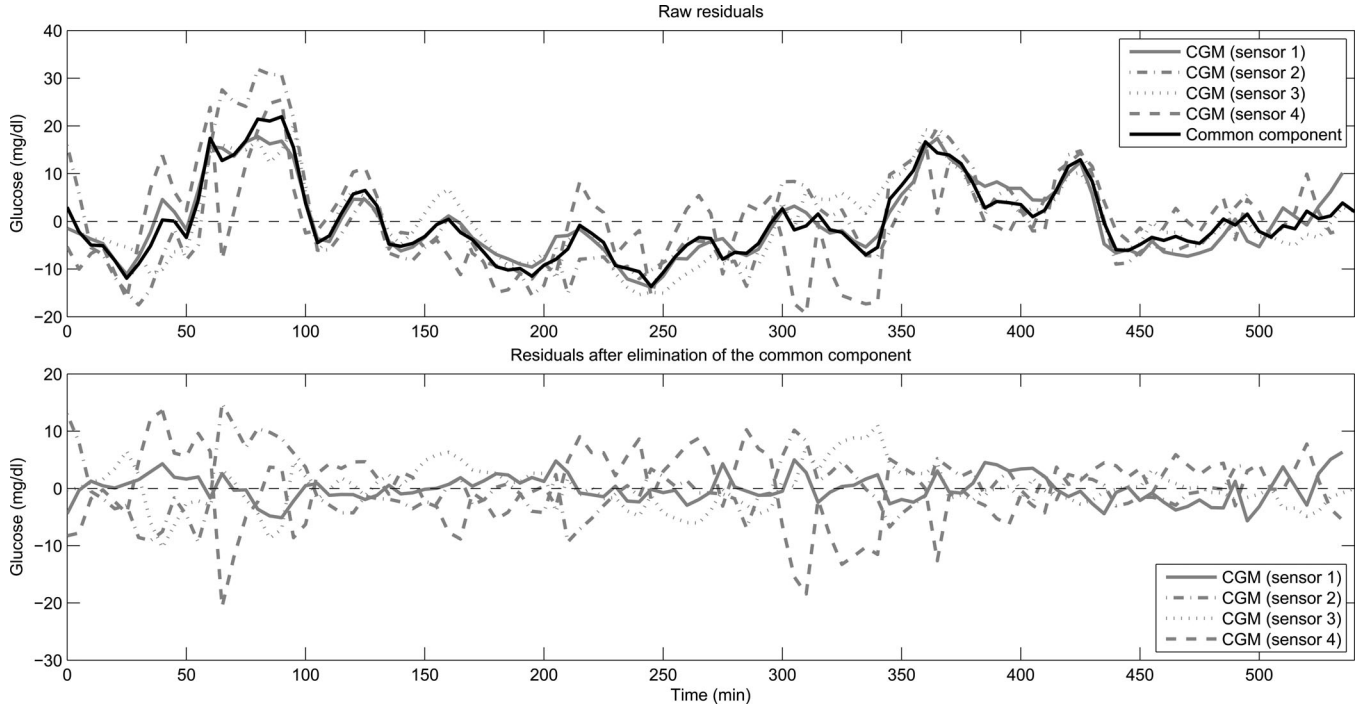

Fig. 5. Same representative example of Fig. 1. (Top) raw residuals of the four CGM sensors. A significant positive correlation among the four traces is evident. The common component, obtained by using (11), is also plotted in black. (Bottom) Residuals after the elimination of the common component.

subject of Fig. 1. We can observe that residuals are highly correlated. For instance, focusing on sensors 1–3, the correlation coefficients r^2 calculated among them are greater than 0.8. The common component is highly visible (plotted with a black line). This support the fact that the description given by models used for the BG-to-IG diffusion process and calibration are suboptimal. In particular, we might speculate that most critical model is that describing the BG-to-IG diffusion process, since the calibration error has been analyzed in details in this paper. The bottom panel of Fig. 5 shows the same residuals of the top panel after the elimination of the common component: the correlation among the residuals is significantly reduced, e.g., among sensors 1–3 it is now $r^2 < 0.15$.

As described in Section III, both the common component $\mathrm{cc}(t)$ and the residuals $\hat{v}_i(t)$ have been modeled as realizations of AR processes. Fig. 6 illustrates the results of this analysis. For each of the two signals, the top panel reports the counts of time series in which that specific order has been selected as optimal, while the bottom panel shows the estimated variance of the process. It appears clear that both signals can be optimally described by an AR model of order 2 [AR(2)]. For what concerns the variance of the processes, comparing the two bottom panels of Fig. 6, it is very interesting to note how the variance of the common component is significantly greater than the one relative to the measurement noise (median values are 57.6 and 31.5 $\mathrm{mg}^2/\mathrm{dl}^2$, respectively, $p = 0.0016$ Wilcoxon Ranksum test). This result is key to better understand the measurement noise component in CGM sensors. In fact, without multiple sensor data, all the variance on residuals res_i would have been associated with the measurement noise v_i (as in [31] and [34]). However, multiple sensor data analysis evidenced that only 33% of the variance

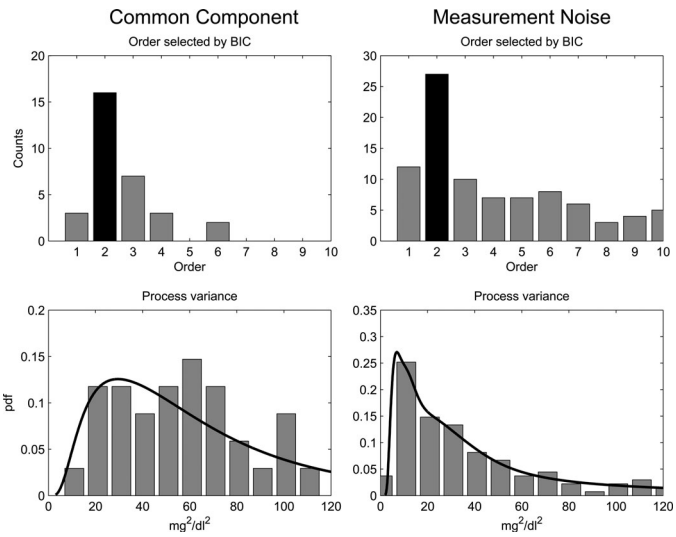

Fig. 6. Results of the analysis on common component (panels on the left side) and measurement noise time series (panels on the right side). For each one, the histogram on the top reports the counts of time series in which that specific order has been selected as optimal (in black the most selected order), while the histogram on the bottom the distribution of the estimated variances of the time series.

can be associated with the measurement noise, while the large amount is due to suboptimal modeling of previous steps of the analysis.

In order to validate the goodness of the AR models identified in the previous analysis, we applied the Anderson–Darling test to the prediction-error time series $e(t)$ (details on the test are reported in the Appendix). Numerically, 73.5% of common

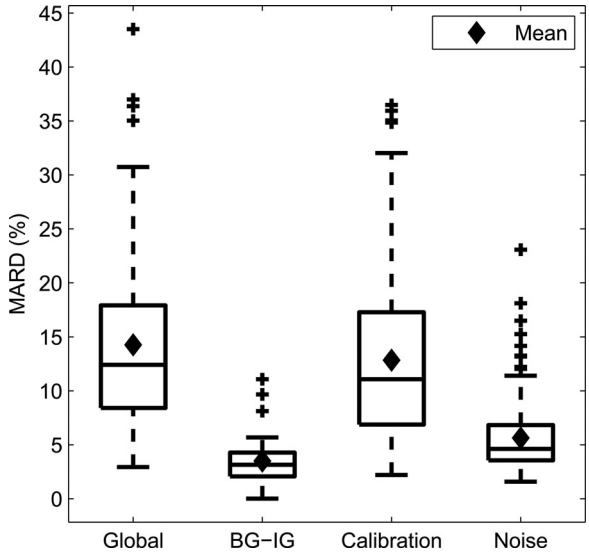

Fig. 7. Boxplots of MARD values of original CGM traces, calculated comparing BG versus CGM (global), and of all the other key components of sensor error: BG-to-IG kinetics (BG–IG), calibration errors, and drift in time of sensor sensitivity (calibration), and measurement noise (noise). The diamond (◊) is the mean value.

components time series and 81.5% of the measurement noise time series passed Anderson–Darling test, meaning that the description of these processes through an AR(2) is satisfactory and reliable.

Starting from the aforementioned results, we also identified population AR(2) processes for both the common component and the measurement noise, which resulted

$$\mathrm{cc}(t) = 1.23cc(t-1) - 0.3995cc(t-2) + w_{\mathrm{cc}}(t) \quad (13)$$

with $w_{\mathrm{cc}}(t) = \mathcal{N}(0, 11.3\ \mathrm{mg}^2/\mathrm{dl}^2)$, and

$$\hat{v}(t) = 1.013\hat{v}(t-1) - 0.2135\hat{v}(t-2) + w(t) \quad (14)$$

with $w(t) = \mathcal{N}(0, 14.45\ \mathrm{mg}^2/\mathrm{dl}^2)$. In particular, focusing on the measurement noise $v(t)$ of (14), this process can be seen as the measurement noise characterizing the Dexcom SEVEN Plus sensor and can be used to take into account its statistical description within algorithms for the processing of CGM that require it, e.g., the Bayesian denoising algorithm of [26] when implemented on this type of sensor.

D. Sensor Error Dissection

Thanks to the dissection of sensor error into physiological and technological components, we can quantify the relative contribution to the overall sensor error. The metric used is the mean absolute relative difference (MARD), which is widely used in the CGM community [25]. Fig. 7 illustrates the boxplots of MARD values of global error and the three key components of sensor error: BG-to-IG diffusion process (BG–IG), calibration errors and drift in time of sensor sensitivity (calibration), and measurement noise (noise). The average global MARD, calculated comparing CGM and BG data, was 14.2%, in line with similar studies performed in the literature with the same sensor [25], [27]. The average MARD associated with the BG-to-IG diffusion process, calculated comparing IG and BG time series, is 3.5%, evidencing that the contribution of this kind of error on the total amount is modest. Then, we calculated the MARD of IG versus cIG time series, i.e., the error associated with the deviation due to calibration errors and drift-in-time of sensor sensitivity, which resulted on average 12.8%. In the end, we calculated the average MARD due to the measurement noise, which is 5.6%, greater than the BG-to-IG error, but significantly lower than the calibration error. We can observe that, among the three principal errors, the one related to calibration and drift-in-time is the most important and the most critical in determining CGM sensor accuracy. In fact, this MARD value is very close to the total amount of the error ($p = ns$), while contributions of BG-to-IG diffusion process and measurement noise are significantly lower ($p < 0.001$ in both cases). Thus, this analysis suggests that, to improve accuracy of the sensor, more work on calibration and drift-in-time is needed.

VI. Conclusion

Modeling of CGM sensor error and dissecting the components of CGM inaccuracy are important in several applications. For instance, a reliable description of the measurement noise enables the design of optimal digital filters for denoising; a precise assessment of the BG-to-IG kinetics is important for enhancement and calibration methods; finally, an acceptable description of the sensor error is crucial in the type 1 diabetes simulator used to develop and test *in silico* closed-loop control algorithms for AP. Available literature models of CGM sensor error were not able to describe all sensor error variability which can be observed in CGM time series, mainly because the dataset on which these models have been identified did not allow any better modeling (single-input BG time series, single-output CGM time series). The availability of multiple CGM profiles simultaneously measured in parallel to reference BG in the same subject allows us to improve the quantitative knowledge on sensor error.

The modeling methodology for sensor error description we proposed in this paper is more detailed than those presented in the literature, especially for what concerns the description of calibration errors and sensor drift-in-time. In particular, sensor drift-in-time was explicitly considered for the first time. Furthermore, being based on the availability of multiple CGM sensor data, not only the parameters of the model are more robustly estimated, but also a quantification of errors due to models can be derived (what we labeled as common component).

The modeling procedure has been tested on a dataset of 19 type 1 diabetic subjects (monitored twice) in which $n = 4$ simultaneous Dexcom SEVEN Plus CGM time series were available for each patient together with BG references frequently measured via laboratory instrument. Results evidenced that the proposed modeling methodology is able to: perform a precise and reliable estimation of model parameters, especially for what concerns the time constant τ of the BG-to-IG diffusion process; evidence the presence of drift-in-time on CGM time series, thus better characterizing the calibration error; and return a more

precise estimation of the measurement noise, since dynamics that are not related to measurement noise (i.e., the common component) are properly eliminated (and subtracted) before the identification step. In addition, the dissection of sensor error evidenced that, in general, the CGM inaccuracy is mostly due to errors in calibration and sensor drift.

This paper opens the door for further developments. For instance, should the raw sensor signal be accessible, a finer dissection of sensor error components could be investigated. Another step forward could come from physiological studies of the BG-to-IG kinetics obtained with novel experiments employing tracers. Moreover, placing the sensors in sites different from the abdomen may help in better investigating the BG-to-IG kinetics and how the sensor error is correlated with the application site (not possible with the Dexcom SEVEN Plus used in [23], since is FDA approved only for the abdomen). Furthermore, with reference to the assumption of piecewise constant parameters m, l, a_{ik}, and b_{ik} of the calibration error model (see the *Remark* at the end of Section III), even if the absence of calibrations is a prerequisite of our analysis (a calibration would introduce a nonlinearity in the parameters), the short duration of the monitoring hindered the possibility of understanding if and how these submodels evolve in time. Should datasets with longer duration (e.g., seven days) become available, time-varying polynomials (in which parameters can change over sensor life time) could be investigated. Finally, exploiting the common component to retune structure/order/parameters of BG-to-IG kinetics and calibration error models could be investigated by developing *ad hoc* iterative estimation techniques.

We conclude remarking that the approach here presented to derive the components of CGM sensor error is general and is applicable to other sensors, including the recently launched Dexcom G4 Platinum, when datasets with frequent BG reference measurements and multiple CGM data, like the one employed for validation in this paper, are available.

APPENDIX

We present here the Anderson–Darling test. The test is applied on prediction-error time series $e(t)$ of the target time series under analysis to test if the model used to fit the data well describes them. In our case, the model is an AR process and $e(t)$ is derived by inverting the AR process transfer function (previously identified) and using as input the target time series. If the identified AR model well describes the target time series, the sequence of $e(t)$ values will be white noise, i.e., the autocorrelation function $\rho_e(k)$, with $k = 1, 2, \ldots$, will be 1 for $k = 0$, and 0 elsewhere. To verify this, accordingly to the Anderson–Darling test, we assume as null hypothesis H_0 that $e(t)$ is white noise. Then, we estimate the autocorrelation function values $\hat{\rho}_e(k)$ and we check their statistical description, i.e., $\hat{\rho}_e(k) = \mathcal{N}(0, 1/N)$ for $k \neq 0$. Having fixed the significance value $\alpha = 5\%$, the $(-\beta, \beta)$ interval in which $(1 - \alpha)\%$ values of $\rho_e(k)$ falls is calculated. Finally, if the number of $\hat{\rho}_e(k)$ values lying outside the interval $(-\beta, \beta)$ is lower than α, the null hypothesis H_0 is accepted.

ACKNOWLEDGMENT

The authors would like to thank C. Agnoletto (M.Sc. in Bioengineering at the University of Padova) for her help in the implementation of part of the algorithms.

REFERENCES

[1] M. Cox, "An overview of continuous glucose monitoring systems," *J. Pediatr. Health Care*, vol. 23, no. 5, pp. 344–347, 2009.

[2] G. McGarraugh, "The chemistry of commercial continuous glucose monitors," *Diabetes Technol. Ther.*, vol. 11, suppl 1, pp. 17–24, Jun. 2009.

[3] M. Joubert and Y. Reznik, "Personal continuous glucose monitoring (CGM) in diabetes management: Review of the literature and implementation for practical use," *Diabetes Res. Clin. Pract.*, vol. 96, pp. 294–305, Jun. 2012.

[4] J. E. Lane, J. P. Shivers, and H. Zisser, "Continuous glucose monitors: Current status and future developments," *Curr. Opin. Endocrinol. Diabetes Obes.*, vol. 20, pp. 106–111, Apr. 2013.

[5] W. V. Tamborlane, R. W. Beck, B. W. Bode, B. Buckingham, H. P. Chase, R. Clemons, R. Fiallo-Scharer, L. A. Fox, L. K. Gilliam, I. B. Hirsch, E. S. Huang, C. Kollman, A. J. Kowalski, L. Laffel, J. M. Lawrence, J. Lee, N. Mauras, M. O'Grady, K. J. Ruedy, M. Tansey, E. Tsalikian, S. Weinzimer, D. M. Wilson, H. Wolpert, T. Wysocki, D. Xing, H. P. Chase, R. Fiallo-Scharer, L. Messer, V. Gage, P. Burdick, L. Laffel, K. Milaszewski, K. Pratt, E. Bismuth, J. Keady, M. Lawlor, B. Buckingham, D. M. Wilson, J. Block, K. Benassi, E. Tsalikian, M. Tansey, D. Kucera, J. Coffey, J. Cabbage, H. Wolpert, G. Shetty, A. Atakov-Castillo, J. Giusti, S. O'Donnell, S. Ghiloni, I. B. Hirsch, L. K. Gilliam, K. Fitzpatrick, D. Khakpour, T. Wysocki, L. A. Fox, N. Mauras, K. Englert, J. Permuy, B. W. Bode, K. O'Neil, L. Tolbert, J. M. Lawrence, R. Clemons, M. Maeva, B. Sattler, S. Weinzimer, W. V. Tamborlane, B. Ives, J. Bosson-Heenan, R. W. Beck, K. J. Ruedy, C. Kollman, D. Xing, J. Jackson, M. Steffes, and J. M. Bu, "Continuous glucose monitoring and intensive treatment of type 1 diabetes," *N. Engl. J. Med.*, vol. 359, pp. 1464–1476, Oct. 2008.

[6] D. Rodbard, "Glycemic variability: Measurement and utility in clinical medicine and research—One viewpoint," *Diabetes Technol. Ther.*, vol. 13, pp. 1077–1080, Nov. 2011.

[7] F. J. Service, "Glucose variability," *Diabetes*, vol. 62, pp. 1398–1404, May 2013.

[8] B. P. Kovatchev, D. J. Cox, L. A. Gonder-Frederick, and W. Clarke, "Symmetrization of the blood glucose measurement scale and its applications," *Diabetes Care*, vol. 20, pp. 1655–1658, Nov. 1997.

[9] W. Clarke and B. Kovatchev, "Statistical tools to analyze continuous glucose monitor data," *Diabetes Technol. Ther.*, vol. 11 suppl 1, pp. 45–54, Jun. 2009.

[10] S. Guerra, G. Sparacino, A. Facchinetti, M. Schiavon, C. D. Man, and C. Cobelli, "A dynamic risk measure from continuous glucose monitoring data," *Diabetes Technol. Ther.*, vol. 13, pp. 843–852, Aug 2011.

[11] G. McGarraugh and R. Bergenstal, "Detection of hypoglycemia with continuous interstitial and traditional blood glucose monitoring using the FreeStyle Navigator Continuous Glucose Monitoring System," *Diabetes Technol. Ther.*, vol. 11, pp. 145–150, Mar. 2009.

[12] A. Kamath, A. Mahalingam, and J. Brauker, "Methods of evaluating the utility of continuous glucose monitor alerts," *J. Diabetes Sci. Technol.*, vol. 4, pp. 57–66, Jan. 2010.

[13] M. H. Jensen, T. F. Christensen, L. Tarnow, E. Seto, M. Dencker Johansen, and O. K. Hejlesen, "Real-time hypoglycemia detection from continuous glucose monitoring data of subjects with type 1 diabetes," *Diabetes Technol. Ther.*, Apr. 2013.

[14] G. Sparacino, A. Facchinetti, and C. Cobelli, ""Smart" continuous glucose monitoring sensors: On-line signal processing issues," *Sens. (Basel)*, vol. 10, no. 7, pp. 6751–6772, 2010.

[15] B. W. Bequette, "Continuous glucose monitoring: Real-time algorithms for calibration, filtering, and alarms," *J. Diabetes Sci. Technol.*, vol. 4, pp. 404–418, Mar. 2010.

[16] C. Zecchin, A. Facchinetti, G. Sparacino, and C. Cobelli, "Reduction of number and duration of hypoglycemic events by glucose prediction methods: A proof-of-concept in silico study," *Diabetes Technol. Ther.*, vol. 15, pp. 66–77, Jan. 2013.

[17] C. Cobelli, E. Renard, and B. Kovatchev, "Artificial pancreas: Past, present, future," *Diabetes*, vol. 60, pp. 2672–2682, Nov. 2011.

[18] R. Hovorka, J. M. Allen, D. Elleri, L. J. Chassin, J. Harris, D. Xing, C. Kollman, T. Hovorka, A. M. Larsen, M. Nodale, A. De Palma, M. E. Wilinska, C. L. Acerini, and D. B. Dunger, "Manual closed-loop insulin delivery in children and adolescents with type 1 diabetes: A phase 2 randomised crossover trial," *Lancet*, vol. 375, pp. 743–751, Feb. 2010.
[19] M. Breton, A. Farret, D. Bruttomesso, S. Anderson, L. Magni, S. Patek, C. Dalla Man, J. Place, S. Demartini, S. Del Favero, C. Toffanin, C. Hughes-Karvetski, E. Dassau, H. Zisser, F. J. Doyle, G. De Nicolao, A. Avogaro, C. Cobelli, E. Renard, and B. Kovatchev, "Fully integrated artificial pancreas in type 1 diabetes: modular closed-loop glucose control maintains near normoglycemia," *Diabetes*, vol. 61, pp. 2230–2237, Sep. 2012.
[20] C. Cobelli, E. Renard, B. P. Kovatchev, P. Keith-Hynes, N. Ben Brahim, J. Place, S. Del Favero, M. Breton, A. Farret, D. Bruttomesso, E. Dassau, H. Zisser, F. J. Doyle, S. D. Patek, and A. Avogaro, "Pilot studies of wearable outpatient artificial pancreas in type 1 diabetes," *Diabetes Care*, vol. 35, pp. e65–e67, Sep. 2012.
[21] S. J. Russell, F. H. El-Khatib, D. M. Nathan, K. L. Magyar, J. Jiang, and E. R. Damiano, "Blood glucose control in type 1 diabetes with a bihormonal bionic endocrine pancreas," *Diabetes Care*, vol. 35, pp. 2148–2155, Nov. 2012.
[22] M. Phillip, T. Battelino, E. Atlas, O. Kordonouri, N. Bratina, S. Miller, T. Biester, M. A. Stefanija, I. Muller, R. Nimri, and T. Danne, "Nocturnal glucose control with an artificial pancreas at a diabetes camp," *N. Engl. J. Med.*, vol. 368, pp. 824–833, Feb. 2013.
[23] J. R. Castle, A. Pitts, K. Hanavan, R. Muhly, J. El Youssef, C. Hughes-Karvetski, B. Kovatchev, and W. K. Ward, "The accuracy benefit of multiple amperometric glucose sensors in people with type 1 diabetes," *Diabetes Care*, vol. 35, pp. 706–710, Apr. 2012.
[24] B. Kovatchev, S. Anderson, L. Heinemann, and W. Clarke, "Comparison of the numerical and clinical accuracy of four continuous glucose monitors," *Diabetes Care*, vol. 31, pp. 1160–1164, Jun. 2008.
[25] E. R. Damiano, F. H. El-Khatib, H. Zheng, D. M. Nathan, and S. J. Russell, "A comparative effectiveness analysis of three continuous glucose monitors," *Diabetes Care*, vol. 36, pp. 251–259, Feb. 2013.
[26] A. Facchinetti, G. Sparacino, and C. Cobelli, "Online denoising method to handle intraindividual variability of signal-to-noise ratio in continuous glucose monitoring," *IEEE Trans. Biomed. Eng.*, vol. 58, no. 9, pp. 2664–2671, Sep. 2011.
[27] A. Facchinetti, G. Sparacino, S. Guerra, Y. M. Luijf, J. H. Devries, J. K. Mader, M. Ellmerer, C. Benesch, L. Heinemann, D. Bruttomesso, A. Avogaro, and C. Cobelli, "Real-time improvement of continuous glucose monitoring accuracy: The smart sensor concept," *Diabetes Care*, vol. 36, pp. 793–800, Apr. 2013.
[28] A. Facchinetti, G. Sparacino, and C. Cobelli, "Enhanced accuracy of continuous glucose monitoring by online extended Kalman filtering," *Diabetes Technol. Ther.*, vol. 12, pp. 353–363, May 2010.
[29] B. P. Kovatchev, M. Breton, C. D. Man, and C. Cobelli, "In silico preclinical trials: A proof of concept in closed-loop control of type 1 diabetes," *J. Diabetes Sci. Technol.*, vol. 3, pp. 44–55, Jan. 2009.
[30] C. Dalla Man, F. Micheletto, D. Lv, M. Breton, B. Kovatchev, and C. Cobelli, "The UVA/Padova type 1 diabetes simulator: New features," *J. Diabetes Sci. Technol.*, vol. 7, no. 6, 2013.
[31] M. Breton and B. Kovatchev, "Analysis, modeling, and simulation of the accuracy of continuous glucose sensors," *J. Diabetes Sci. Technol.*, vol. 2, pp. 853–862, Sep. 2008.
[32] K. Rebrin, G. M. Steil, W. P. van Antwerp, and J. J. Mastrototaro, "Subcutaneous glucose predicts plasma glucose independent of insulin: Implications for continuous monitoring," *Amer. J. Physiol.*, vol. 277, pp. E561–E571, Sep. 1999.
[33] A. Facchinetti, G. Sparacino, and C. Cobelli, "Modeling the error of continuous glucose monitoring sensor data: Critical aspects discussed through simulation studies," *J. Diabetes Sci. Technol.*, vol. 4, pp. 4–14, Jan. 2010.
[34] D. J. Lunn, C. Wei, and R. Hovorka, "Fitting dynamic models with forcing functions: application to continuous glucose monitoring in insulin therapy," *Stat. Med.*, vol. 30, pp. 2234–2250, Aug. 2011.
[35] S. Guerra, A. Facchinetti, G. Sparacino, G. D. Nicolao, and C. Cobelli, "Enhancing the accuracy of subcutaneous glucose sensors: A real-time deconvolution-based approach," *IEEE Trans. Biomed. Eng.*, vol. 59, no. 6, pp. 1658–1669, Jun. 2012.
[36] A. Kamath, A. Mahalingam, and J. Brauker, "Analysis of time lags and other sources of error of the DexCom SEVEN continuous glucose monitor," *Diabetes Technol. Ther.*, vol. 11, pp. 689–695, Nov. 2009.

Andrea Facchinetti was born in Padova, Italy, on July 27, 1981. He received the Doctoral degree (Laurea) *cum laude* in information engineering and the Ph.D. degree in bioengineering, both from the University of Padova, Padova, Italy, in 2005 and 2009, respectively.

He is currently a Postdoctoral Researcher at the University of Padova, Padova, Italy. His current scientific interests include optimal filtering, Bayesian estimation, deconvolution techniques, and neural networks applied to signal processing problems. He has published more than 30 papers in international peer-reviewed journals.

Simone Del Favero was born in Pieve di Cadore (BL), Italy, on November 7, 1982. He received the *summa cum laude* degree (Hons.) in automation engineering from the University of Padova, Padova, Italy, in 2006 and the Ph.D. degree in information science and technology in March 2010.

His research interests include estimation, learning and dynamical-system identification, with applications to sensor networks and physiological systems, especially the insulin–glucose system. He is currently a Postdoctoral Researcher at the University of Padova and he works within an international team to the designing, development, and clinical testing of minimally invasive artificial pancreas based on subcutaneous glucose sensing and subcutaneous insulin infusion.

Giovanni Sparacino was born in Pordenone, Italy, on November 11, 1967. He received the Doctoral degree in electronics engineering *cum laude* from the University of Padua, Padua, Italy, in 1992 and the Ph.D. degree in biomedical engineering from the Polytechnic of Milan, Milan, Italy, in 1996.

Since 1997, he has been with the University of Padua, Padua, Italy: from 1997 to 1998, he was a Research Engineer at the Faculty of Medicine; from 1999 to 2004, he was an Assistant Professor at the Faculty of Engineering; since 2005, he has been an Associate Professor of Biomedical Engineering at the Faculty of Engineering. His scientific interests include deconvolution and parameter estimation techniques for the study of physiological systems, linear and nonlinear biological time series analysis, estimation of evoked potentials (single-trial, improved averaging, steady-state responses), continuous glucose monitoring (calibration, denoising, and prediction). On these topics, he published more than 60 papers in international peer-reviewed journals and tens of other contributions in books and conference proceedings.

Jessica R. Castle was born in Veneta, OR, USA, on February 11, 1978. She received the graduation degree in biology from the Robert D. Clark Honors College, University of Oregon, Eugene, OR, USA, in 2000, and the *summa cum laude* degree from Oregon Health & Science University, Portland, OR, USA, in 2004.

She completed internal medicine residency and endocrinology fellowship training at Oregon Health & Science University, where she is currently an Assistant Professor. The focus of her research is treating patients with type 1 diabetes using an artificial pancreas system. She also treats patients at the Harold Schnitzer Diabetes Health Center.

W. Kenneth Ward received the degree in medicine from the University of Colorado, School of Medicine, Denver, CO, USA, in 1978. He completed internal medicine residency at the University of Colorado, Denver, and the endocrinology and metabolism research fellowship at the University of Washington School of Medicine and Seattle VA Medical Center, Seattle, WA, USA.

Currently, he holds faculty positions at Oregon Health & Science University and Legacy Research Institute, both in Portland, OR, USA. From 1998–2008, he was a Chief Science Officer at iSense. He is a member of the JDRF-supported Artificial Pancreas Consortium and has written multiple scientific papers and patents in the areas of amperometric glucose sensing (chemistry, membranes, interference, polymers, sensing algorithms, redundancy) and clinical studies of the artificial endocrine pancreas. In March 2010, with Dr. Castle, Dr. El Youssef and others, his team published a paper on the novel use of glucagon and insulin in controlling glycemia in persons with type 1 diabetes. He also directs a JDRF-sponsored project to create a pumpable, liquid formulation of glucagon.

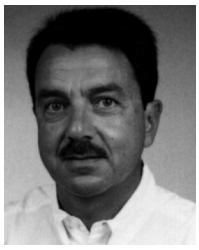

Claudio Cobelli (S'67–M'70–SM'97–F'03) was born in Bressanone (Bolzano), Italy, on February 21, 1946. He received the Doctoral degree (Laurea) in electrical engineering from the University of Padova, Padova, Italy, in 1970.

From 1970 to 1980, he was a Research Fellow with the Institute of System Science and Biomedical Engineering, National Research Council, Padova, Italy. From 1973 to 1975 and 1975 to 1981, he was an Associate Professor of Biological Systems at the University of Florence and an Associate Professor of Biomedical Engineering at the University of Padova, respectively. In 1981, he became a Full Professor of Biomedical Engineering at University of Padova. Since 2000, he has been an Affiliate Professor with Bioengineering at the University of Washington, Seattle, WA, USA. From 2000 to 2009, he was the Chairman of the Graduate Program in Biomedical Engineering. From 2000, he is the Chairman of the Ph.D. Program in Bioengineering at the University of Padova. His main research activity is in the field of modeling and identification of physiological systems, especially endocrine-metabolic systems. He has published more than 300 papers in internationally refereed journals. He is coeditor of *Carbohydrate Metabolism: Quantitative Physiology and Mathematical Modeling* (Chichester, U.K.: Wiley, 1981), *Modeling and Control of Biomedical Systems* (Oxford, U.K.: Pergamon Press, 1989), and *Modeling Methodology for Physiology and Medicine* (New York, NY, USA: Academic Press, 2000). He is coauthor of *The Mathematical Modeling of Metabolic and Endocrine Systems* (New York, NY, USA: Wiley, 1983), *Tracer Kinetics in Biomedical Research: from Data to Model* (London, U.K.: Kluwer Academic/Plenum Publishers, 2001), and *Introduction to Modeling in Physiology and Medicine* (San Diego, CA, USA: Academic Press, 2008).

Dr. Cobelli is currently an Associate Editor of IEEE TRANSACTION ON BIOMEDICAL ENGINEERING. He is on the Editorial Board of *American Journal of Physiology: Endocrinology and Metabolism*, and of *Journal of Diabetes Science & Technology*. In the past, he has been an Associate Editor of Mathematical Biosciencies and on the Editorial Board of Control Engineering Practice, Diabetes, Nutrition & Metabolism, Diabetologia and *American Journal of Physiology: Modeling in Physiology*. He has been Chairman (1999–2004) of the Italian Biomedical Engineering Group, Chairman (1990–1993 and 1993–1996) of IFAC TC on Modeling and Control of Biomedical Systems, and IEEE EMBS AdCom Member (2008–2009). In 2010, he received the Diabetes Technology Artificial Pancreas Research Award. He is Fellow of the Biomedical Engineering Society and the American Institute for Medical and Biological Engineering.